

Semi-Autonomous Mobile Search and Rescue Robot for Radiation Disaster Scenarios

Simon Schwaiger^{*1}, Lucas Muster^{*1,2}, Georg Novotny¹, Michael Schebek¹,
Wilfried Wöber¹, Stefan Thalhammer¹ and Christoph Böhm¹

Abstract—This paper describes a novel semi-autonomous mobile robot system designed to assist search and rescue (SAR) first responders in disaster scenarios. While robots offer significant potential in SAR missions, current solutions are limited in their ability to handle a diverse range of tasks. This gap is addressed by presenting a system capable of (1) *autonomous navigation and mapping*, allowing the robot to autonomously explore and map areas affected by catastrophic events, (2) *radiation mapping*, enabling the system to triangulate a radiation map from discrete radiation measurements to aid in identifying hazardous areas, (3) *semi-autonomous substance sampling*, allowing the robot to collect samples of suspicious substances and analyze them onboard with immediate classification, and (4) *valve manipulation*, enabling teleoperated closing of valves that control hazardous material flow. This semi-autonomous approach balances human control over critical tasks like substance sampling with efficient robot navigation in low-risk areas. The system is evaluated during three trials that simulate possible disaster scenarios, two of which have been recorded during the European Robotics Hackathon (EnRiCH). Furthermore, we provide recorded sensor data as well as the implemented software system as supplemental material through a GitHub repository: <https://github.com/TW-Robotics/search-and-rescue-robot-IROS2024>.

I. INTRODUCTION

In the context of search and rescue (SAR), robots are deployed to aid emergency teams in responding faster and more efficiently in case of a disaster scenario [1]–[4]. Robots are used in dangerous environments to collect important information about the area of operation [5]–[7] to keep human first responders away from a potentially hazardous environment and minimise their exposure to harmful substances. These robotic systems need to handle diverse tasks, such as exploration and mapping of disaster zones [8], localizing hazardous material [9], and solving manipulation tasks [10]. However, SAR robots with a varying skill-set are not a standard piece of equipment of SAR response teams, therefore, their potential is not fully realized [11].

Recent advances have been made in the implementation of mapping [12], hazardous material localization [13], [14],

^{*}Equal contribution

This work was supported by the Austrian Research Promotion Agency (FFG) through the research project UGV-ABC-Probe (FFG project Call 2020) and the Austrian Armed Forces.

¹Simon Schwaiger, Lucas Muster, Georg Novotny, Michael Schebek, Wilfried Wöber, Stefan Thalhammer and Christoph Böhm are with the Faculty of Industrial Engineering, University of Applied Sciences Technikum Wien, 1200 Vienna, Austria schwaige@technikum-wien.at, muster@technikum-wien.at

²Lucas Muster is with the University of Natural Resources and Life Sciences, Department of Biotechnology, Institute for Computational Biology, Muthgasse 18, 1190 Vienna, Austria

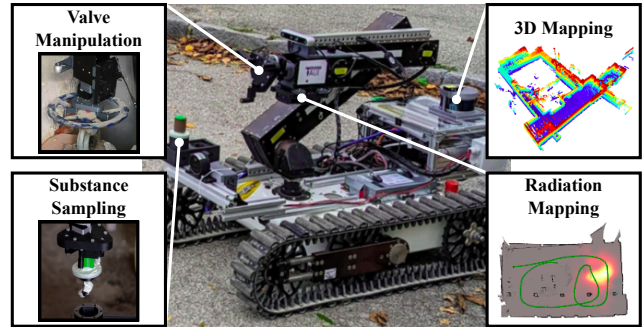


Fig. 1: **Robot capabilities.** The robot system solves four tasks on one platform to assist first responders in disaster scenarios: Autonomous navigation and mapping, radiation mapping, semi-autonomous substance sampling and valve manipulation.

and manipulation tasks [3]. Those systems address and solve individual tasks. However, for efficient deployment, their capabilities need to be combined on a single platform. Our presented system performs a diverse set of tasks in areas affected by catastrophes based on requirements set by real world problems encountered by the Austrian Armed Forces. Our robot, as depicted in Fig. 1, fulfills these requirements by being capable of

- autonomously navigating and exploring the vicinity and creating a map of the robot’s surrounding geometry,
- measuring radiation and triangulating a radiation map,
- taking samples of substances on the floor in a semi-autonomous fashion with subsequent on-board analysis, and
- closing valves that control the flow of hazardous material.

This paper advances the current state of the art in SAR robotics by designing and implementing a semi-autonomous mobile robot system. Our experiments show, that the robot provides these capabilities in a unified platform. Therefore, our robot potentially improves support for rescue teams during disasters.

The remainder of this paper is structured as follows. Sec. II presents recent advances in autonomous SAR systems. Sec. III provides a methodological overview of the SAR robot and the fulfilled tasks, while Sec. IV discusses robot hardware and software. Sec. V describes the robot’s evaluation in three scenarios and Sec. VI summarizes our

research and provides an outlook on future work.

II. RELATED WORK

The increased interest in mobile robots aiding in SAR missions motivates researchers and companies to create solutions for the tasks encountered in these scenarios. These tasks range from teleoperated exploration or inspection to semi-autonomous mission execution. Challenges stemming from given real-world problems allow the evaluation of mobile robotic systems in safe and controlled environments. The result of all those efforts are fast to deploy and easy to use systems for real-world disaster sites.

A. Competitions and Challenges

Past and current competitions and challenges emulate a single task or a whole series of tasks (mission) found in real-world problems. These tasks can vary in scale, from enclosed rooms to whole sites, and their complexity, from exploring and inspection to fully autonomous interactions with the environment.

Conferences often hold competitions on a smaller scale with single task requirements, e.g., ICRA 2023 BARN Challenge¹. Bigger challenges that contain whole missions for mobile robots such as the DARPA Subterranean (SubT) Challenge², Total Autonomous Robot for Gas and Oil Sites (ARGOS), or The European Land Robot Trial (ELROB)³ often originate from the need of practical SAR solutions. Hence, they provide a valuable proving ground for SAR robots. Our robotic system was present at the European Robotics Hackathon (EnRicH)⁴ in 2023 and data was collected to evaluate the effectiveness of the system. During the challenge, a hazardous material incident response operation was staged.

B. Mobile Robotic Systems for Search and Rescue

One of the first uses of mobile robots in SAR missions at the World Trade Center (WTC) disaster site 2001 is documented in [1]. Tethered tracked robot vehicles with cameras that are teleoperated helped rescuers on site. The team conducted multiple runs with the following tasks: (1) searching for victims, (2) searching for faster excavation paths, (3) structural inspection, and (4) detection of hazardous materials. These robots were able to enter spaces too small or dangerous for humans or rescue dogs. Another example of mobile robotic systems aiding humans was showcased 2011 in Japan during the Fukushima nuclear accident. Researchers deployed the teleoperated mobile robotic platform TALON equipped with a radiation sensor [2]. The heavy radiation prohibited humans from entering the area, therefore, a robot was used to localize radiation sources, using light detection and ranging (LiDAR) depth information and radiation measurements.

¹<https://www.icra2023.org/competitions>

²<https://www.darpa.mil/program/darpa-subterranean-challenge>

³<https://www.elrob.org/>

⁴<https://enrich.european-robotics.eu/>

Over the last two decades, researchers came up with many solutions to mobile robots in SAR missions. One example of such a robotic system is the work by the authors of [10] which proposed a remotely operated mobile robot for radiation mapping and semi-autonomous sampling of radioactive sources. Many robots [9], [14]–[16] solely focusing on radiation mapping were presented by the research community. These systems use discrete maps of the contaminated area and navigate through user predefined way-points or coverage areas. The robots measure radiation levels during the operation and generate a radiation map. This map can be used by the users themselves or navigation packages use them to avoid sources. [17] is an example of autonomous exploration (coverage planning) and environmental measuring based on behavior trees for task execution. This robot participated at the EnRicH in 2019. Almost all solutions rely on the user selecting points of interest, while the robotic system presented in this work uses exploration to autonomously determine interesting spots to complete the radiation map.

An alternative to ground vehicles in the context of SAR robotics are uncrewed areal vehicle (UAV). [18], [19] automate radiation mapping using flying autonomous systems, allowing for coverage of bigger areas. However, UAVs are limited by their maximum take-off weight and flight time.

Most solutions in radiation mapping lack the capability of manipulation, a needed skill in SAR missions. This is emphasized by the application shown in research [3], [20], [21]. All robots are able to interact with their environment, e.g., removing potential obstacles with a robotic manipulator or evacuate victims from the disaster site by carrying them away. These robots are teleoperated, therefore, control and manipulation happens based on direct user input or a list of way-points.

Our approach incorporates semi-autonomous manipulation tasks, e.g., sampling and analysis of potentially hazardous materials, to aid disaster response.

In the current state of the art, research gaps are identified with regard to robots' abilities to perform diverse tasks consisting of reconnaissance as well as manipulation. Furthermore, systems incorporating manipulation act in a teleoperated manner and lack autonomy. We address these gaps by implementing reconnaissance in the form of geometry and radiation mapping as well as autonomous exploration. Additionally, our system is capable of performing two manipulation tasks, i.e., substance sampling and valve manipulation.

III. METHOD

The presented SAR robot's capabilities are depicted in the form of a high-level overview in Fig. 2. The used tracked ground vehicle [22] has a five degree of freedom (DOF) arm mounted onto the chassis for manipulation tasks. The mobile platform is equipped with sensors and an end-effector that enable it to complete required tasks in a semi-autonomous fashion. Two LiDAR sensors and an inertial measurement unit (IMU) allow for 2D and 3D simultaneous localisation and mapping (SLAM) using LiDAR-odometry and mapping

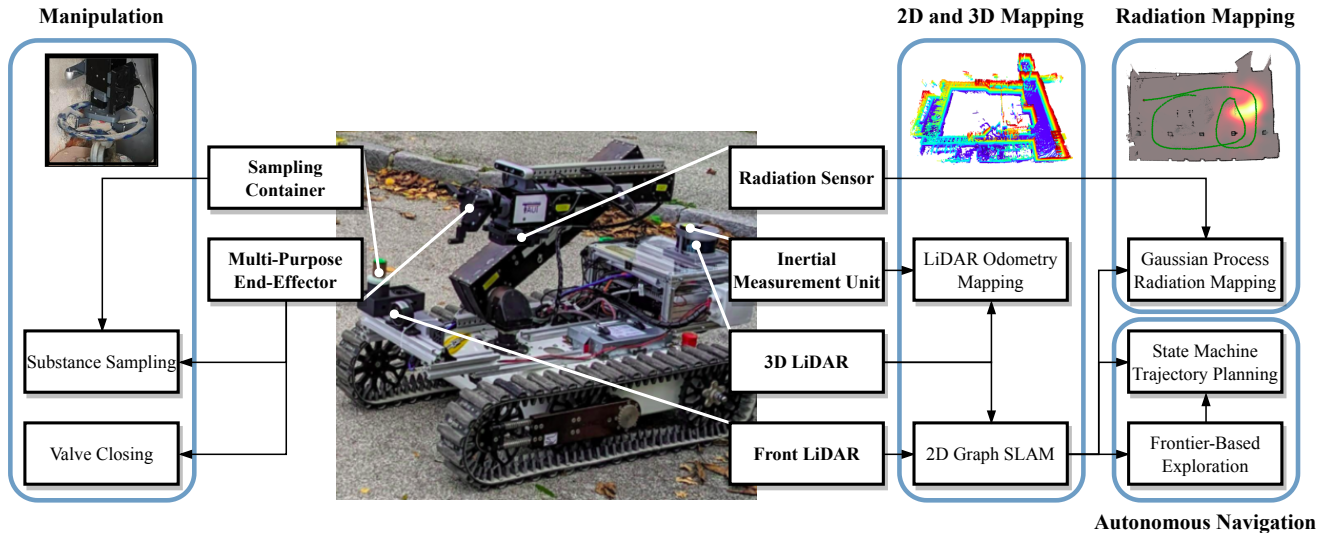


Fig. 2: **Functional system overview.** The proposed system aims to provide 2D and 3D mapping, radiation mapping, autonomous navigation and manipulation capabilities (blue rounded border) for SAR missions. The figure depicts the data flow between functional units, sensors and the multi-purpose end-effector.

in 3D and a graph-based SLAM in 2D. The generated 2D map serves as the basis for autonomous navigation. Robot movement is planned using a finite state machine with recovery behaviors. A frontier-based exploration algorithm proposes goal poses, that allow the robot to extend its discovered map. The generated 2D map is fused with measurements from a radiation sensor in order to perform radiation mapping. The setup is complemented by a multi-purpose end-effector that enables sampling of substances encountered during a mission using a Raman spectrometer. Furthermore, the end-effector is capable of manipulating valves that control the flow of hazardous material.

A. 2D and 3D Mapping

When implementing the system, we adhered to the conventions set by the Robot Operating System (ROS) [23] and its reference robots [24] to enable compatibility with existing software implementations. The mapping setup consists of a separate 3D as well as a more efficient 2D SLAM system running on a industrial PC. This approach was chosen to enable autonomous navigation without relying on the computationally expensive 3D mapper. The utilised 2D mapper was chosen based on its wide adoption as the by default supported mapper in ROS 2 [25].

The 3D mapper is used for visualization with the intent of providing the robot’s non-technical users with a more realistic representation of the robot’s environment compared to a 2D map. 3D mapping is performed on data from the 3D LiDAR and IMU [26]. The combination of LiDAR and IMU is more robust than LiDAR-only mapping, especially when handling aggressive motion and sudden robot rotation [27]. Since a separate 2D SLAM is the basis of the navigation system, the robot behavior is unaffected by disabling online 3D mapping in order to save performance.

B. Autonomous Navigation Stack

Autonomous navigation is achieved by planning a trajectory from the current pose to a goal pose based on the map and robot pose estimated by the 2D mapper. Layered costmaps [28] have been established as the standard approach to mobile robot trajectory planning in ROS [29]. However, to deal with track slippage and make planning more robust, costmap-based trajectory planning is performed using hierarchical finite state machines that are complemented by custom recovery behaviors that are activated if the robot does not successfully navigate to a desired pose. The implemented recovery behaviors allow the robot to autonomously (1) move away in case of a collision and (2) clear the local costmap if no path can be planned in the robot’s direct vicinity.

The goal pose is either provided by a human operator or the frontier-based exploration module, which proposes goal poses for the robot to navigate to in order to expand the mapped area. Therefore, autonomous and teleoperated modes are intelligently blended to achieve semi-autonomous behavior. Control signals given by the human operator are favored over control signals given by the exploration or trajectory planning modules. This approach allows the robot’s users to interrupt autonomous behavior by providing direct control signals or setting goal poses using the graphical user interface.

The robot’s standard behavior is also interrupted if it loses connection to the operator PC. If the operator can not be communicated with, for example, due to a wireless communication breakdown, a routine is executed that preempts exploration and navigates the robot back towards its starting pose.

C. Radiation Mapping

The mapping of nuclear radiation is based on count data gathered by a Geiger counter. While the mapping of such radiation was previously done by estimating the posterior predictive distribution described by a Poisson distribution [30], autonomous mapping using robots is a challenging task due to the presence of both, process and sensor noise. A radiation mapping pipeline optimized for autonomous mobile robots is proposed in [31]. The authors apply non-parametric Gaussian process regression (GPR) [32] using adapted kernels to map the radiation based on Geiger counts. In this context, a Gaussian process (GP) models the spatial distribution of radiation and interpolates between sampling points.

Our proposed approach for mapping is inspired by [10], however, we extend their work by applying GP to mapping, as seen in [31]. The developed radiation mapping pipeline combines the mobile robot’s current pose (see Sec. IV-B) with count data gathered by the digital Geiger counter. At each time step t , the gathered radiation count data c_t is synchronized with the robot’s pose x_t estimated by the 2D mapper [25]. The training data \mathcal{D} describes the gathered poses and count data.

In a similar manner to [31], the map is estimated by defining the posterior predictive distribution $p(c_{new}|x_{new}, x_{1:t}, c_{1:t}) = p(c_{new}|x_{new}, \mathcal{D})$ relying on GPR with radial base function kernels [32]. Hence, for each location (i, j) in the map m , we can estimate the radiation using Eq. (1), where the functions $GP_\mu(\cdot)$ and $GP_\Sigma(\cdot)$ describe the prediction functions of the GP.

$$\forall i, j \in m, p(c_{i,j}|x_{i,j}, \mathcal{D}) \approx \mathcal{N}(GP_\mu(x_{i,j}, \mathcal{D}), GP_\Sigma(x_{i,j}, \mathcal{D})) \quad (1)$$

The mapping procedure described in Eq. (1) is applied in an offline manner, i.g., after the robot has explored unknown environments.

D. Manipulation System

The manipulation system consists of an industrial robotic arm with five DOF that is complemented by a custom three-finger gripper as end-effector. The end-effector is designed to perform two diverse tasks, namely closing valves as well as grasping the probe used for sampling. The gripper’s tool center point (TCP) is located along the robot arm’s fifth axis in order to turn valves and correctly orient samples into the analysis tray (see Fig. 3).

The end-effector grasps a probe used to absorb potentially harmful substances for on-board analysis. This probe consists of an interface to the gripper in cylindrical form and a glass wool swab. The construction allows the swab to be correctly rotated towards the sensor for substance analysis.

Up to two probes can be stored in a storage tray on the SAR robot. One additional probe slot is present at the back of the robot, where samples of substances are examined by a Raman spectrometer.

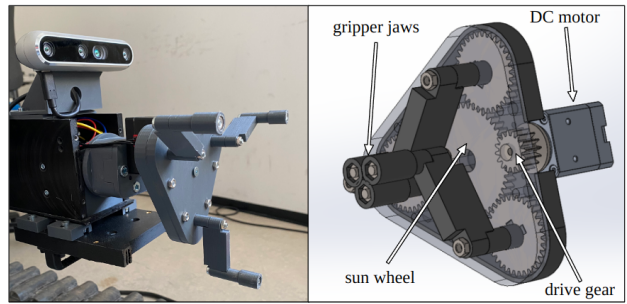


Fig. 3: **Custom gripper for valve manipulation.** The left part of the figure shows a real image of the custom gripper and the right part shows the modelled end-effector with highlighted individual parts.

IV. IMPLEMENTATION DETAIL

As presented in [33], our implementation utilizes a synergistic integration of Docker containers⁵ to encapsulate software packages, systemd service management⁶ to start, stop and restart groups of containers, and the Cockpit monitoring tool⁷ for monitoring software packages running within each systemd service.

Docker containers encapsulate and isolate our robot’s individual software components. This approach allows each software package’s diverse dependencies to be managed individually. It enables us to set up software in a portable and hardware-agnostic manner, while selectively allowing communication between software components when needed.

Systemd, a service management system, automates and manages the lifecycle of Docker containers in groups that represent the main stages (sensing, perception, mapping, exploration, navigation) of the SAR robot’s data processing pipeline. Systemd ensures that these groups are reliably started, stopped, and restarted as needed based on whether or not the robot’s core drivers are running. The setup utilizes systemd template unit files that start Docker compose files, allowing the concurrent management of multiple container instances.

The Cockpit monitoring tool provides a comprehensive view of system status, including the health and activity of both Docker containers and systemd services, facilitating efficient monitoring by human operators. This approach allows for immediate identification and troubleshooting of potential problems, aiding in the SAR robot’s continuous availability. Furthermore, Cockpit allows Docker containers and systemd services to be started, stopped and restarted manually using the graphical user interface. In combination with having software components encapsulated, the user interface allows for parts of the software stack to be restarted during a mission without shutting down the whole system. This functionality is not natively supported by ROS when using the robot control pipeline using a launchfile.

⁵<https://www.docker.com/>

⁶<https://systemd.io/>

⁷<https://cockpit-project.org/>

The remainder of this section details the specific components of the robotic system, including utilized hardware, the software implementing autonomous navigation and the deployed endeffector.

A. Hardware

The SAR robot’s built-in industrial PC features an *Intel i7 7700T* CPU, *Nvidia GTX 1050 Ti* GPU and 32 GB of system memory. An *Nvidia Jetson Xavier NX 16GB* single board computer interfaces with the front cameras. A *Realsense D455* is mounted to the robot’s arm for teleoperated manipulation, while a *Realsense L515* serves as the front LiDAR used to fill the main 3D LiDAR’s scan. The main 3D LiDAR is a *Velodyne VLP-16*, while the utilized IMU is a *LORD 3DMGX5-GNSS/INS*. Radiation is measured using a *Flir Identifinder R300* sensor, while the sample analysis sensor has the model name *Thermo Scientific FirstDefender RMX Handheld Chemical Identification*.

B. Navigation and Mapping Software

The system leverages ROS 1 (version Noetic) on the industrial PC, while the single board PC runs on ROS 2 (version Humble). Slam Toolbox [25] serves as the system’s 2D mapper, while trajectory planning is performed by Move Base Flex [29]. LIO-SAM [26] performs 3D mapping based on 3D LiDAR and IMU measurements. Explore Lite⁸ generates goal poses, where the map depicting the discovered area can be expanded.

Autonomous and teleoperated operation modes are automatically switched between using priority-based multiplexers. When switching from a signal source with a higher priority to a lower priority (e.g., switching from a teleoperation-based command velocity to a velocity generated by the trajectory planner) switching occurs with a pre-defined cooldown to prevent the robot base from oscillating between conflicting control signals.

Two multiplexers are deployed across the pipeline. The first multiplexer switches between command velocities generated by the operator (teleoperation) and the autonomous navigation stack. The second multiplexer switches the goal pose between the following sources in descending priority: (1) Go home routine, (2) planning preemption, (3) user interface and (4) explorer. Go home routine depicts the stored home pose that the robot navigates to in case the connection to the operator is interrupted, while planning preemption depicts a node that preempts trajectory planning if the operator performs teleoperation. In this context, user interface refers to goal poses that the operator can send by clicking on the 2D map in the user interface and explorer refers to goalposes proposed by the map exploration module.

C. End-effector

The SAR robot is equipped with a custom end-effector that is capable of both, closing valves as well as grasping the probe used for sampling. Manipulated objects are automatically centered through the gripper’s kinematics and can

therefore be rotated using the robot arm’s fifth axis that is aligned with the end-effector’s TCP. After accounting for the reduction in the planetary gearbox, the resulting gripping force of 80 Newtons on the TCP is generated by a *Robotis XM430-W350* servo motor. Assuming centered placement of the TCP along a valve’s rotation axis, the end-effector can manipulate valves of up to 160 millimeters in diameter by grasping them from the outside. Additionally, larger valves with gaps between the center of rotation and handle can be grasped inside the valve’s handle.

V. EXPERIMENTS

Our robot was evaluated during trials in the Tritolwerk nuclear biological chemical (NBC) and disaster relief training area as well as the EnRicH European Robotics Hackathon. The Tritolwerk NBC and disaster relief training area, situated in Eggendorf, Austria, serves as a training ground for the Austrian Armed Forces and various emergency response organizations. It includes ruins and bunker facilities, which serve as our setting for simulating diverse disaster scenarios. EnRicH is hosted at the decommissioned nuclear power plant in Zwentendorf, Austria and aims to simulate catastrophic events and evaluate robots’ ability to navigate hazardous environments and locate survivors.

A. Experimental Setup

We test the robot’s ability to perform the four tasks outlined in Sec. I, which revolve around mapping the geometry and radiation in the robot’s environment, taking samples of substances for the Raman spectrometer to analyze and closing valves in a semi-autonomous manner. The following chapters present experiments conducted to demonstrate the robot’s capability to perform these tasks in the following scenarios:

- **Scenario 1: Tritolwerk main production hall**
This test location is two stories tall and features pillars and scaffolding within the room. During the trial, a radiation source is placed near one of the hall’s exits. The radiation source is partly occluded using bricks to test the radiation mapping’s ability to estimate the spread of radioactive emissions from the discrete radiation measurements.
- **Scenario 2: Indoor navigation in nuclear power plant (EnRicH training area)**
This test consists of navigation through hallways and the power plant’s turbine rooms. The area features narrow hallways connecting multiple rooms, resulting in more rooms compared to scenario 1. However, no radiation source is present, therefore, no radiation map is plotted in Fig. 5.
- **Scenario 3: Radiation source pattern**
During this scenario, the robot is teleoperated to move towards an unobstructed radiation source in an open space. The robot’s trajectory follows a flower-shaped pattern to imitate how human disaster responders triangulate radiation sources. The scenario is located outside near the nuclear power plant Zwentendorf.

⁸<https://github.com/hrnr/m-explore>

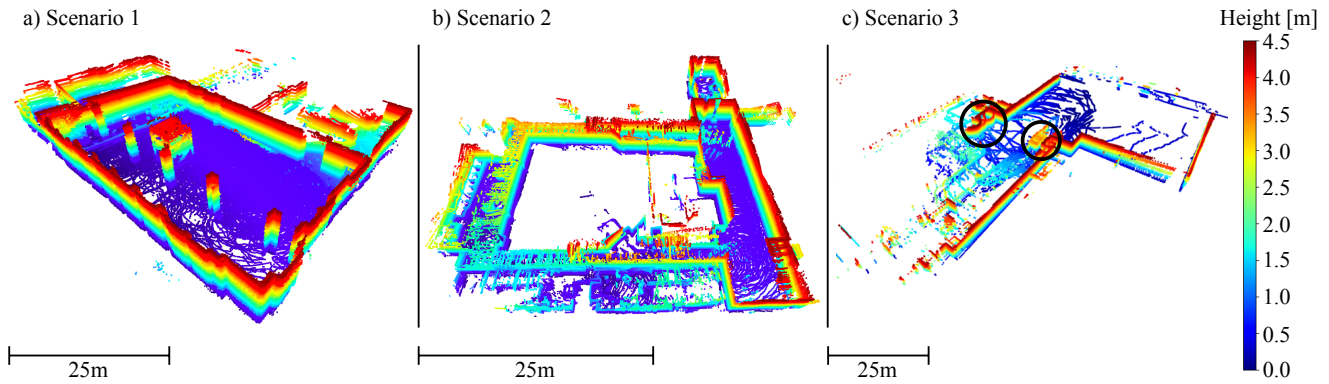


Fig. 4: **Autonomous Mapping results.** The 3D maps resulting from online mapping are visualized as pointclouds. a), b) and c) correspond to scenarios 1, 2 and 3. The legend indicating map height using the colormap applies to all maps. In c), improperly mapped geometry is highlighted by two black circles.

B. Autonomous Mapping

Fig. 4 plots the 3D maps generated from all three scenarios. In scenario 1 (Fig. 4a), details, such as the scaffolding in the middle of the room, belts used to secure the scaffolding as well as the barrier at the top entrance of the hall are properly captured and visualized by the system. The neighboring rooms are incomplete since the mission only involves the main hall.

Scenario 2's area (see Fig. 4b) consists of narrow corridors, which results in a denser pointcloud compared to scenario 1. The hallways form a loop, where loop closure is correctly applied by the 3D mapper. The turbine rooms on the bottom of the plot are not fully shown in the map, because the robot is too wide to navigate into these rooms.

Scenario 3 (see Fig. 4c) shows an open outside area. Contrary to Fig. 4a) and Fig. 4b), the resulting map shows deficiencies highlighted using black circles. In these areas, the same geometry has been mapped multiple times due to

a drift in odometry. This behavior is most likely caused by the direct sunlight experienced during the trials, which introduces significant noise into the LiDAR measurements. Similar to scenarios 2 and 3, [8] also provide maps of the nuclear power plant Zwentendorf recorded during EnRich, however, they omit the section depicted in Fig. 4c).

C. Radiation Mapping

Fig. 5 presents the 2D map used for navigation (black) and the robot trajectory (green) overlaid onto the radiation map (yellow shading) for scenario 1 (Fig. 5a) and scenario 3 (Fig. 5b). The resulting heatmap represents a triangulation of each radiation source based on discrete radiation measurements within the 2D map. Fig. 5a) shows the dampening of radioactive emissions to the top right of the radiation source. This dampening corresponds to the locations where bricks were placed to partially occlude the radiation source. The trajectory shown in Fig. 5b) shows the robot circling

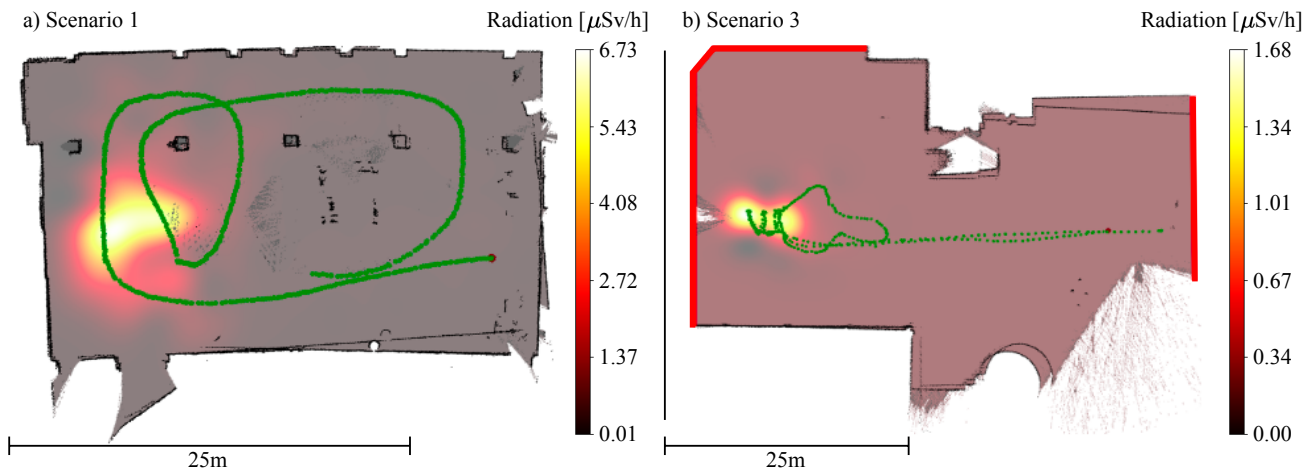


Fig. 5: **Radiation mapping results.** The 2D map (black) is overlaid with the robot's trajectory (green) and the estimated radiation map (yellow shading) during scenario 1, depicted in a) and scenario 3, depicted in b). Red borders in b) indicate map truncation to zoom into relevant parts of the map.

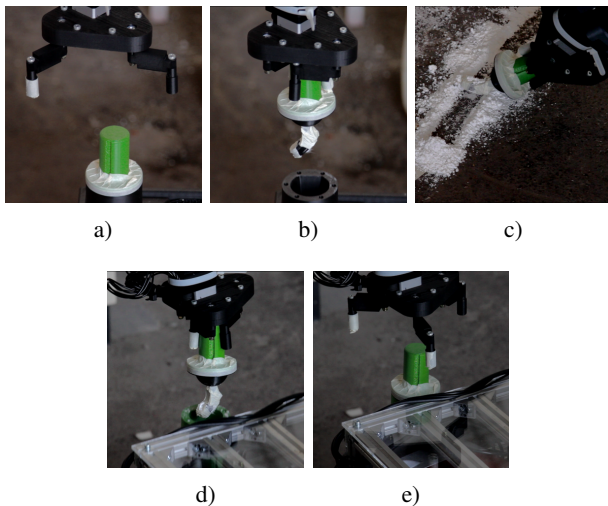


Fig. 6: **Semi-autonomous sampling sequence.** The sampling process consists of the following poses: a) ready to get probe from storage, b) grasp probe, c) swipe substance, d) ready to place sample, and e) sample placed in analysis tray.

the radiation source at different distances. This teleoperated trajectory aims to imitate how human first responders manually triangulate the position of radiation sources by circling the estimated position of the radiation source in a pattern resembling a flower. Scenario 2 is omitted from Fig. 5 because there is no radiation source present during the trial.

D. Semi-Autonomous Sampling

The goal of the semi-autonomous sampling procedure is to collect solid powder-like as well as fluid substances using one of the stored probes and to analyze them on-board. Fig. 6 presents a series of autonomous routines that are called sequentially by the operator to sample a powdered substance in front of the robot. The process includes a) preparation to get a probe from storage, b) probe grasping, c) swiping of the probe through the sampled substance, d) preparation to place the sample, and e) probe placement in the analysis tray. The robot arm trajectory between the poses presented in Fig. 6 is planned in a manner that prevents direct fly-over of the contaminated probe. This approach prevents the sampled substance from trickling from the probe onto the robot chassis while it is moved from the sampling pose to the analysis tray.

E. Teleoperated Valve Manipulation

Fig. 7 presents the robot performing the valve closing task in scenario 1. The SAR robot manipulates a tank's 100 millimeter output valve by gripping the valve from the outside.

VI. CONCLUSIONS

In this paper, we present a semi-autonomous search and rescue (SAR) mobile robot system, aimed at assisting first responders in disaster scenarios. It fulfils four main tasks in one combined solution: (1) autonomous exploration and

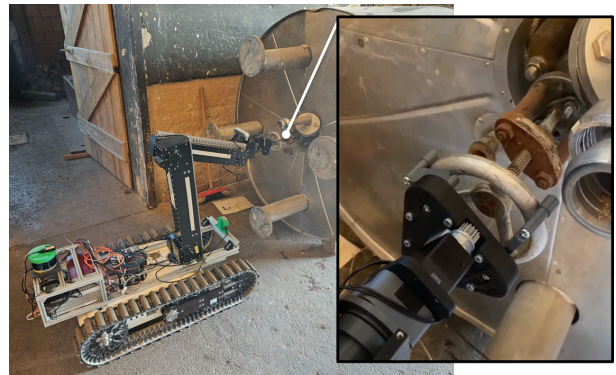


Fig. 7: **Valve manipulation.** The SAR mobile robot manipulates a tank's output valve at Tritolwerk, Eggenburg, Austria. The gripper is closed partially to match the valve's 100 mm outer diameter ensuring proper grip of the handle.

mapping of unknown areas, (2) triangulation of a map from discrete radiation measurements, (3) sampling and analysis of encountered substances in a semi-autonomous manner, and (4) teleoperated manipulation of valves that control the flow of hazardous substances. The system is based on a tracked robot base with a five degree of freedom (DOF) robot arm for manipulation and uses 2D, 3D and radiation mapping pipelines for autonomous navigation as well as visualization of the robot environment to the human operators. Semi-autonomous robot navigation is achieved using priority-based multiplexing of control signals, while the sampling and valve manipulation tasks are solved using a combination of prerecorded routines and teleoperation. The system was evaluated at a disaster response training site as well as at the European Robotics Hackathon (EnRicH) to show its ability to perform the required tasks.

Future work on the presented system intends to improve perception capabilities, especially in direct sunlight by tightly coupling the camera's image data to the light detection and ranging (LiDAR) odometry and mapping pipeline. Furthermore, the level of autonomy during valve manipulation can be increased by incorporating methods for vision-guided arm control, such as visual servoing, into the robot control pipeline.

REFERENCES

- [1] R. R. Murphy, "Trial by fire [rescue robots]," *IEEE Robotics & Automation Magazine*, vol. 11, no. 3, pp. 50–61, 2004.
- [2] K. Ohno, S. Kawatsuma, T. Okada, E. Takeuchi, K. Higashi, and S. Tadokoro, "Robotic control vehicle for measuring radiation in fukushima daiichi nuclear power plant," in *2011 IEEE International Symposium on Safety, Security, and Rescue Robotics*. IEEE, 2011, pp. 38–43.
- [3] K. Berns, A. Nezhadfar, M. Tosa, H. Balta, and G. D. Cubber, "Unmanned ground robots for rescue tasks," in *Search and Rescue Robotics*. Rijeka: IntechOpen, 2017, ch. 4.
- [4] H. Chitikena, F. Sanfilippo, and S. Ma, "Robotics in search and rescue (sar) operations: An ethical and design perspective framework for response phase," *Applied Sciences*, vol. 13, no. 3, 2023.
- [5] G. Lunghi, R. Marin, M. Di Castro, A. Masi, and P. J. Sanz, "Multimodal human-robot interface for accessible remote robotic interventions in hazardous environments," *IEEE Access*, vol. 7, pp. 127 290–127 319, 2019.

- [6] M. P. Manuel, M. Faied, and M. Krishnan, "A novel lora lpwan-based communication architecture for search & rescue missions," *IEEE Access*, vol. 10, pp. 57 596–57 607, 2022.
- [7] D. H. Stolfi, M. R. Brust, G. Danoy, and P. Bouvry, "Uav-ugv-umv multi-swarms for cooperative surveillance," *Frontiers in Robotics and AI*, vol. 8, 2021.
- [8] J. Bedkowski, "Open source, open hardware hand-held mobile mapping system for large scale surveys," *SoftwareX*, vol. 25, p. 101618, 2024.
- [9] K. Groves, E. Hernandez, A. West, T. Wright, and B. Lennox, "Robotic exploration of an unknown nuclear environment using radiation informed autonomous navigation," *Robotics*, vol. 10, no. 2, 2021.
- [10] R. Guzman, R. Navarro, J. Ferre, and M. Moreno, "Rescuer: Development of a modular chemical, biological, radiological, and nuclear robot for intervention, sampling, and situation awareness," *Journal of Field Robotics*, vol. 1–15 (2015), 06 2015.
- [11] J. P. Queralta, J. Taipalmaa, B. Can Pullinen, V. K. Sarker, T. Nguyen Gia, H. Tenhunen, M. Gabbouj, J. Raitoharju, and T. Westlund, "Collaborative multi-robot search and rescue: Planning, coordination, perception, and active vision," *IEEE Access*, vol. 8, pp. 191 617–191 643, 2020.
- [12] F. G. Rosas, F. Hoeller, and F. E. Schneider, "Autonomous robot exploration and measuring in disaster scenarios using behavior trees," in *2020 IEEE 10th International Conference on Intelligent Systems (IS)*, 2020, pp. 469–474.
- [13] N. A. Abd Rahman, K. S. M. Sahari, N. A. Hamid, and Y. C. Hou, "A coverage path planning approach for autonomous radiation mapping with a mobile robot," *International Journal of Advanced Robotic Systems*, vol. 19, no. 4, 2022.
- [14] B. Nouri Rahmat Abadi, A. West, M. Nancekievill, C. Ballard, B. Lennox, O. Marjanovic, and K. Groves, "Carma ii: A ground vehicle for autonomous surveying of alpha, beta and gamma radiation," *Frontiers in Robotics and AI*, vol. 10, p. 1137750, 2023.
- [15] N. A. Abd Rahman, K. S. M. Sahari, M. F. A. Jalal, A. A. Rahman, M. I. Abd Adziz, and M. Z. Hassan, "Mobile robot for radiation mapping in indoor environment," in *IOP Conference Series: Materials Science and Engineering*, vol. 785, no. 1. IOP Publishing, 2020, p. 012021.
- [16] A. West, T. Wright, I. Tsitsimpelis, K. Groves, M. J. Joyce, and B. Lennox, "Real-time avoidance of ionising radiation using layered costmaps for mobile robots," *Frontiers in Robotics and AI*, vol. 9, p. 862067, 2022.
- [17] F. G. Rosas, F. Hoeller, and F. E. Schneider, "Autonomous robot exploration and measuring in disaster scenarios using behavior trees," in *2020 IEEE 10th International Conference on Intelligent Systems (IS)*. IEEE, 2020, pp. 469–474.
- [18] G. Christie, A. Shoemaker, K. Kochersberger, P. Tokekar, L. McLean, and A. Leonessa, "Radiation search operations using scene understanding with autonomous uav and ugv," *Journal of Field Robotics*, vol. 34, no. 8, pp. 1450–1468, 2017.
- [19] D. Connor, P. G. Martin, and T. Scott, "Airborne radiation mapping: overview and application of current and future aerial systems," *International Journal of Remote Sensing*, vol. 37, pp. 5953–5987, 12 2016.
- [20] J. Zhao, J. Gao, F. Zhao, and Y. Liu, "A search-and-rescue robot system for remotely sensing the underground coal mine environment," *Sensors*, vol. 17, no. 10, p. 2426, 2017.
- [21] A. Denker and M. C. İşeri, "Design and implementation of a semi-autonomous mobile search and rescue robot: Salvor," in *2017 International Artificial Intelligence and Data Processing Symposium (IDAP)*. IEEE, 2017, pp. 1–6.
- [22] G. A. Novotny and W. Kubinger, "Design and implementation of a mobile search and rescue robot," in *Proceedings of the Joint Austrian Computer Vision and Robotics Workshop*, 2020, pp. 21–26.
- [23] M. Quigley, K. Conley, B. P. Gerkey, J. Faust, T. Foote, J. Leibs, R. Wheeler, and A. Y. Ng, "Ros: an open-source robot operating system," in *ICRA Workshop on Open Source Software*, 2009.
- [24] U. Jahn, D. Heß, M. Stampa, A. Sutorma, C. Röhrig, P. Schulz, and C. Wolff, "A taxonomy for mobile robots: Types, applications, capabilities, implementations, requirements, and challenges," *Robotics*, vol. 9, no. 4, 2020.
- [25] S. Macenski and I. Jambrecic, "Slam toolbox: Slam for the dynamic world," *Journal of Open Source Software*, vol. 6, no. 61, p. 2783, 2021.
- [26] T. Shan, B. Englot, D. Meyers, W. Wang, C. Ratti, and R. Daniela, "Lio-sam: Tightly-coupled lidar inertial odometry via smoothing and mapping," in *IEEE/RSJ International Conference on Intelligent Robots and Systems (IROS)*. IEEE, 2020, pp. 5135–5142.
- [27] D. Lee, M. Jung, W. Yang, and A. Kim, "Lidar odometry survey: recent advancements and remaining challenges," *Intelligent Service Robotics*, Feb 2024.
- [28] D. V. Lu, D. Hershberger, and W. D. Smart, "Layered costmaps for context-sensitive navigation," in *2014 IEEE/RSJ International Conference on Intelligent Robots and Systems*, 2014, pp. 709–715.
- [29] S. Pütz, J. Santos Simón, and J. Hertzberg, "Move base flex a highly flexible navigation framework for mobile robots," in *2018 IEEE/RSJ International Conference on Intelligent Robots and Systems (IROS)*. Madrid, Spain: IEEE, 01.-05. October 2018, pp. 3416–3421.
- [30] A. Abdelhakim, "Machine learning for localization of radioactive sources via a distributed sensor network," *Soft Comput.*, vol. 27, no. 15, p. 10493–10508, 2023.
- [31] A. West, I. Tsitsimpelis, M. Licata, A. Jazbec, L. Snoj, J. Malcolm, and B. Lennox, "Use of gaussian process regression for radiation mapping of a nuclear reactor with a mobile robot," *Scientific Reports*, vol. 11, no. 1, pp. 1–11, 2021.
- [32] C. E. Rasmussen and C. K. I. Williams, *Gaussian processes for machine learning*. MIT Press, 2006.
- [33] G. Novotny, S. Schwaiger, L. Muster, M. Aburaia, and W. Wöber, "On the applicability of docker containers and systemd services for search and rescue applications," in *Proceedings of the Austrian Robotics Workshop*. Johannes Kepler University, 4 2023, pp. 19–24.